Wavelet Analysis of Vortex Breakdown

Jori Elan Ruppert-Felsot[1], Marie Farge[1], and Philippe Petitjeans[2]

[1] Laboratoire de Météorologie Dynamique du CNRS, Ecole Normale Supérieure, Paris jori@lmd.ens.fr
[2] Laboratoire de Physique et Mécanique des Milieux Hétérogènes, UMR CNRS 7636, Ecole Supérieure de Physique et de Chimie Industrielles, Paris phil@pmmh.espci.fr

Abstract. We study the quasi-periodic turbulent bursting of a laboratory produced isolated vortex immersed in laminar flow. We analyze the experimentally measured flow field using orthogonal wavelets to observe the time evolution of the bursting. The discrete wavelet transform is used to separate the flow field into a coherent component, capturing the dynamics and statistics of the vortex during bursting, and an incoherent component, which is structureless and exhibits a different statistical behavior.

Keywords: wavelet, vortex, coherent structure, turbulence, bursting

1 Introduction

It remains an open question as to how the scaling of the classical energy spectrum is formed and what structures can be responsible for the $k^{-5/3}$ scaling in 3D turbulence. Recent experimental studies have focused on a solitary bursting vortex as a source of turbulence, leading to a transient buildup of a turbulent energy cascade [1, 2, 3]. The scaling of the energy spectrum was found to vary from k^{-1} to k^{-2} during the bursting with a $k^{-5/3}$ recovered in the time averaged spectra. The resulting vortex was found to be well approximated by a stretched spiral vortex following Lundgren's model [4], which also predicts a $-5/3$ time-averaged energy spectrum. However, the time evolution of the spectrum is not yet understood and depends upon the specific spatial structure assumed in the vortex model.

Previous studies were conducted using hot-film anemometry [1, 2]. These hot-film measurements have a good time resolution, but require a local Taylor hypothesis to obtain the spatial information necessary to calculate the energy spectrum. More recently particle image velocimetry (PIV) was used to measure the spatial distribution of the velocity field directly, without inferring it from a time series. Simultaneous hot-film probe measurements were used to synchronize the phase of the PIV with the bursting of the vortex. The PIV measurements were then phase averaged to obtain an ensemble average and

Y. Kaneda (ed.), *IUTAM Symposium on Computational Physics and New Perspectives in Turbulence*, 227–232.

to reconstruct an average time record of the bursting. The scaling of the energy spectra in the inertial range based upon the PIV measurements were in good agreement with the previous hot-film measurements [3]. However, the time resolution of the measurements was low and a single burst could not be followed in time. In the current study we use higher time resolution PIV to follow the time behavior of distinct individual bursts.

The vortex under study is a coherent structure that is well localized in space. It is therefore more natural to analyze this flow using a spatially localized set of basis functions rather than a Fourier basis. Wavelets consist of translations and dilations of a compact function and are well localized in physical and spectral space. Wavelets are thus an optimal choice to analyze such turbulent flows that contain features that are well localized in physical space [5]. Indeed, it has been found in simulation [6] and experiment [7] that the dynamics of turbulent flows are dominated by the contribution of a relatively small fraction of wavelet coefficients, the strongest of which correspond to the coherent structures.

2 Experiment

The vortex is produced in a laminar channel flow over a step, shown in Fig. 1. The vortex is intensified and stretched by suction of fluid through the channel walls, transverse to its axis. As the channel flow rate is increased, the vortex becomes increasingly strained. Above a critical channel flow rate the vortex detaches from the walls and eventually breaks down, resulting in a turbulent burst. The Reynolds number at the onset of the burst is estimated as 4000 in [2], based upon the circulation. The resulting turbulent flow is solely due to the bursting because the vortex is initially formed in laminar flow. A new vortex is formed shortly after the burst and this cycle repeats quasi-periodically at intervals of approximately 8 seconds.

We observe the vortex in a plane perpendicular to its axis at the center of the 12 cm × 7 cm cross section channel. Digital images are taken at a

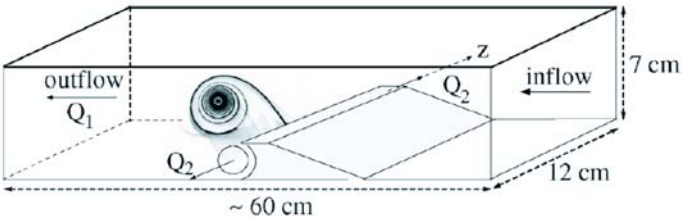

Fig. 1. Schematic of the experiment (from [2]). The vortex initiated by the step (5 mm high) is strained by the channel flow Q_1 and intensified and stretched by the axial suction Q_2 (i.e. the total flow rate through the channel $= Q_1 + 2Q_2$). The values $Q_1 = 12.5$ l min^{-1} and $Q_2 = 7.5$ l min^{-1} were chosen to produce an intense quasi-periodically bursting vortex

resolution of 1600 × 1200 pixels and 30 Hz frame rate. We use a pulsed laser to obtain successive exposures at separations of 1 ms. We then perform PIV on image pairs to measure the velocity field sampled at 15 Hz in a 6.4 cm × 4.8 cm region with 200 × 150 vector resolution. The vorticity component perpendicular to the plane is calculated from the measured 2D velocity field. The PIV measurements are repeated for many vortex breakdown cycles.

3 Wavelet Splitting

We apply wavelet analysis to the vorticity field calculated from the experiment. We follow the technique described in [6] to split the field into two orthogonal components.

The field is cropped to a size 128 × 128 for use with the discrete wavelet transform (DWT) which takes inputs of size $2^n \times 2^n$ (i.e. here $n = 7$). The DWT of a snapshot of the field is calculated using orthogonal wavelets. The optimal threshold is recursively computed as in [6] on the coefficients of the transform. The large amplitude coefficients above the threshold are taken as the coherent component of the field. We calculate their inverse discrete wavelet transform to obtain the coherent field in physical space. The remaining small amplitude coefficients correspond to the incoherent component of the field. Due to the orthogonality of the transform, the total (i.e. the original measured) field is the sum of the coherent and the incoherent fields. This splitting is repeated for each snapshot of the field.

4 Results

An example of splitting the measured vorticity field into coherent and incoherent components is shown in Fig. 2. The coherent field is comprised of a small number of the coefficients of the DWT, only 4% (i.e. 656 of $128 \times 128 = 16384$ total coefficients), and contains 83% of the enstrophy of the total field. The remaining 96% of the coefficients correspond to the incoherent field, containing 17% of the enstrophy of the total field. The coherent field preserves the same structures and features of the total field while the incoherent field is void of coherent spatial structure (see Fig. 2).

A scatter plot of the vorticity versus stream function indicating the spatial coherence of the fields is shown Fig. 3 (a). For a field that contains coherent structures, such as vortices, the distribution is organized along branches, each approximating a sinh function for a single vortex. This is evident in the long arm of the total and coherent fields observed prior to the vortex burst. As the bursting proceeds, this arm contracts and the scatter plot distribution becomes more compact and closer to the origin. The coherent field matches the behavior of the total field, while the incoherent field remains localized near the origin throughout the bursting due to its spatial incoherence.

A time trace of the statistics of the fields is shown in Fig. 3 (b). The field before the burst containing a solitary vortex is characterized by large

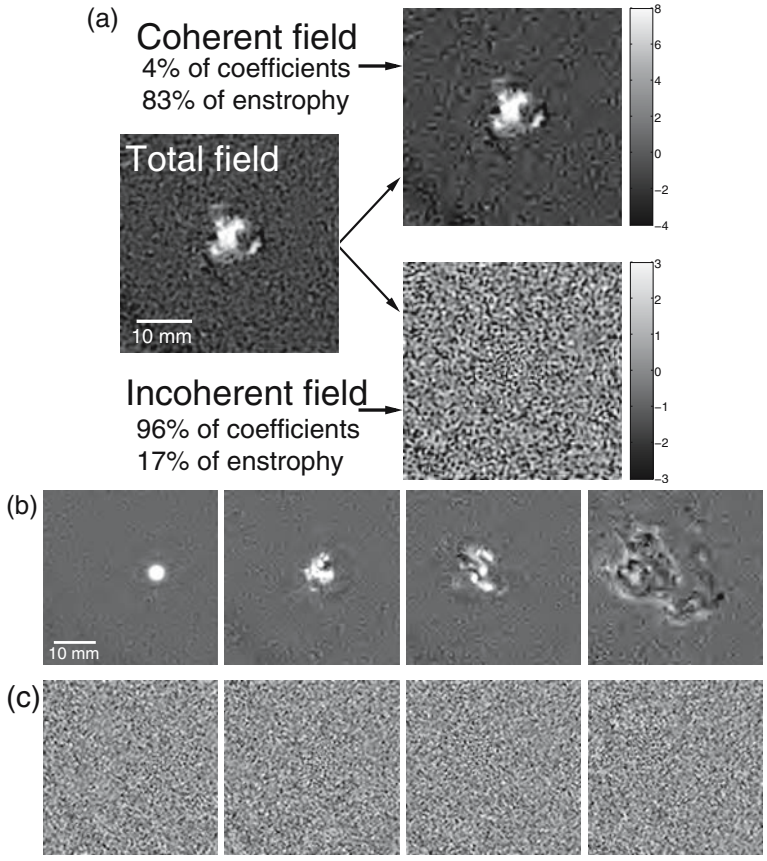

Fig. 2. (**a**) A split of the measured vorticity field into coherent and incoherent fields at the beginning of a burst. Each field snapshot has been renormalized by its standard deviation. (**b**) Time evolution of the coherent field and (**c**) incoherent field. Time proceeds from left to right in intervals of 0.33 seconds while the bursting vortex travels from right to left in the snapshots. The colormaps used for the coherent and incoherent fields are the same as in (**a**)

values of the variance, flatness, and skewness. A rapid decrease is observed during bursting as the vortex looses its coherence and breaks up. The moments return to their large values when a new vortex appears in the field. The statistics of the coherent field follows closely those of the total field, while the incoherent field remains close to Gaussian throughout the bursting. This can be seen in the probability density function (PDF) of the fields taken during the bursting as shown in Fig. 3 (c). The coherent and total fields have a PDF far from Gaussian with a broad and highly skewed distribution. The PDF of the incoherent fields is more symmetric and closer to Gaussian, as shown in the inset of Fig. 3 (c).

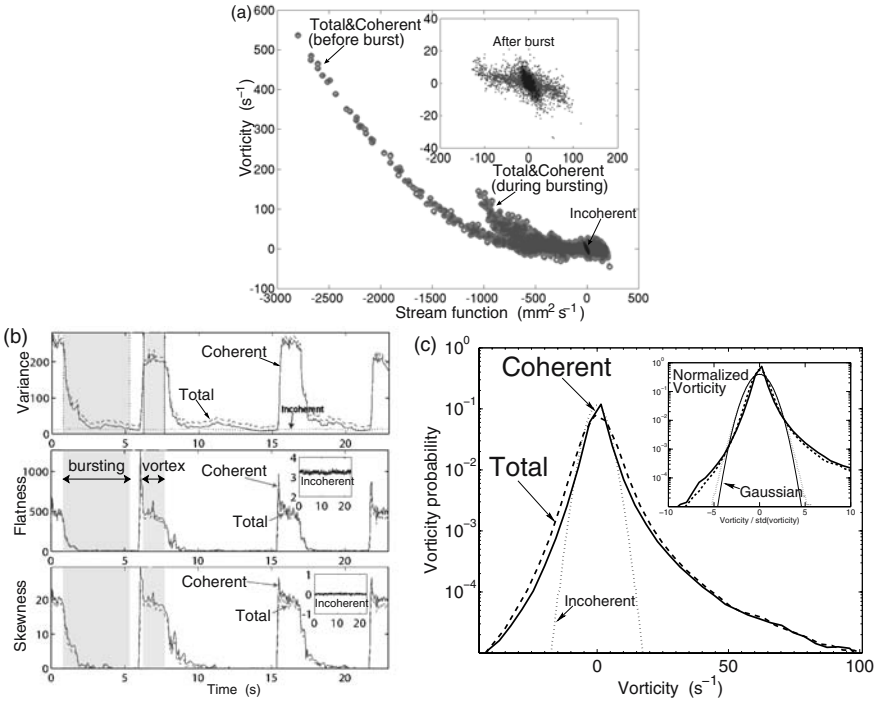

Fig. 3. (**a**) Scatter plot of the stream function versus vorticity showing the coherence of the vorticity field. The total and coherent distributions are nearly indistinguishable while the incoherent remains localized at the origin. The inset shows the fields after the burst. (**b**) Time evolution of the moments of the vorticity field. Plotted are the variance (top), flatness (middle) and skewness (bottom) of the total (dashed line), coherent (solid), and incoherent (dotted) fields during 24 seconds, capturing three bursting events. (**c**) Probability distribution functions of vorticity during the bursting. The inset shows the fields renormalized by their standard deviation

An example of the resulting enstrophy and energy spectra for a single field snapshot is shown in Fig. 4. The coherent spectra match that of the total field and dominate the contribution to the enstrophy in the large and intermediate scales. The incoherent field retains an enstrophy spectra scaling close to that of a random field (k^1 in 2D, corresponding to enstrophy equipartition) and contributes to the total field only in the small scales.

5 Summary

We have split the measured field of a bursting vortex into coherent and incoherent components following the algorithm in [6] using the discrete wavelet transform with orthogonal wavelets. We find that for our experimentally measured field, the coherent component captures the dynamics and statistics of the total field with a relatively small number of coefficients. The incoherent

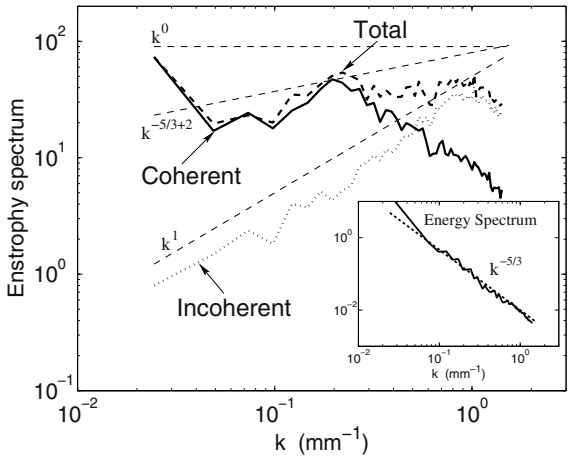

Fig. 4. Enstrophy and energy spectra in the inertial range for a single snapshot of the fields during the bursting. The scaling of the coherent field (solid line) matches the total (dashed) while the incoherent (dotted) remains close to the scaling of Gaussian white noise (k^1 in 2D). The energy spectrum scaling is approximately $k^{-5/3}$

field is void of structure, has near Gaussian statistics, and is relatively insensitive to the bursting.

Future studies will focus on probing the details of the dynamics of the vortex bursting process. We intend to utilize a high speed camera and the continuous wavelet transform to study the time evolution of the bursting and the buildup of the turbulent energy cascade.

References

1. Cuypers Y, Maurel A, Petitjeans P (2003) Phys Rev Lett 91:194502
2. Cuypers Y, Maurel A, Petitjeans P (2004) J Turbul 5:N30
3. Cuypers Y, Maurel A, Petitjeans P (2006) J Turbul 7:N7
4. Lundgren TS (1982) Phys Fluids 25:2193–2203
5. Farge M (1992) Ann Rev Fluid Mech 24:395–457
6. Farge M, Schneider K, Kevlahan N (1999) Phys Fluids 11:2187–2201
7. Ruppert-Felsot JE, Praud O, Sharon E, Swinney HL (2005) Phys Rev E 72:016311